

Extracellular Matrix Dimension and Stiffness Modulate and Remodel Mechano-metabolome of Breast Cancer Cells

Buse Sari¹, Cemilcan Eylem², Emirhan Nemutlu², Matteo D'Este³, Babatunde Okesola⁴, and Burak Derkus¹

¹Ankara University

²Hacettepe University

³AO Research Institute Davos

⁴University of Nottingham

June 7, 2023

Abstract

The stiffness of the tumor microenvironment (TME) is dynamic and drives metabolic reprogramming in cancer cells as a consequence of tumor progression. To demonstrate the possibility to modulate the mechano-metabolomic profile of breast cancers by tuning the mechanical property and dimensionality of extracellular matrices (ECMs), we cultured triple-negative MDA-MB-231 and luminal MCF-7 cells on 2D and in 3D hydrogels based on tyramine functionalized hyaluronic acid (HTA). Using high-throughput metabolomics analyses, we established that we can differentially regulate breast cancer mechano-metabolome. The stiff hydrogels resulted in upregulated lipid and amino acid metabolism along with increasing malignancy and chemoresistancy. Reprogramming in glucose metabolism is primarily observed in cells seeded on 2D hydrogels, whereas modifications in amino acid metabolism is predominant in cells embedded in 3D stiff hydrogels. These findings suggest that matrix stiffness and dimensions have decisive roles in reprogramming breast cancer metabolome, which is the hallmark of breast cancer development and progression.

Extracellular Matrix Dimension and Stiffness Modulate and Remodel Mechano-metabolome of Breast Cancer Cells

Buse Sari¹, Cemil Can Eylem², Emirhan Nemutlu^{2,3}, Matteo D'Este⁴, Babatunde O. Okesola⁵, and Burak Derkus^{1*}

1. Stem Cell Research Lab, Department of Chemistry, Faculty of Science, Ankara University, 06560 Ankara, Turkey
2. Analytical Chemistry Division, Faculty of Pharmacy, Hacettepe University, 06230 Ankara, Turkey
3. Bioanalytic and Omics Laboratory, Faculty of Pharmacy, Hacettepe University, 06230 Ankara, Turkey
4. AO Research Institute Davos, Clavadelerstrasse 8, Davos Platz 7270, Switzerland
5. School of Life Sciences, Faculty of Medicine and Health Sciences, University of Nottingham, Nottingham NG7 2UH, UK *Corresponding author: bderkus@ankara.edu.tr, phone: +90-506-906-97-86 Stem Cell Research Lab, Department of Chemistry, Faculty of Science, Ankara University, 06560 Ankara, Turkey

Key Words: Mechano-oncology, Extracellular matrix, Matrix stiffness, Metabolomics, Breast Cancer

Abstract

The stiffness of the tumor microenvironment (TME) is dynamic and drives metabolic reprogramming in cancer cells as a consequence of tumor progression. To demonstrate the possibility to modulate the mechano-metabolomic profile of breast cancers by tuning the mechanical property and dimensionality of extracellular

matrices (ECMs), we cultured triple-negative MDA-MB-231 and luminal MCF-7 cells on 2D and in 3D hydrogels based on tyramine functionalized hyaluronic acid (HTA). Using high-throughput metabolomics analyses, we established that we can differentially regulate breast cancer mechano-metabolome. The stiff hydrogels resulted in upregulated lipid and amino acid metabolism along with increasing malignancy and chemoresistancy. Reprogramming in glucose metabolism is primarily observed in cells seeded on 2D hydrogels, whereas modifications in amino acid metabolism is predominant in cells embedded in 3D stiff hydrogels. These findings suggest that matrix stiffness and dimensions have decisive roles in reprogramming breast cancer metabolome, which is the hallmark of breast cancer development and progression.

Introduction

Cancer microenvironment and mechanical homeostatic processes are altered from tissue-level modifications to changed cellular signaling pathways associated with mechanotransduction. In breast cancer, the interactions between cell microenvironment and mechanical cues are envisaged as fundamental concepts of breast cancer mechanobiology^{1,2}. Breast cancer progression is generally driven by the biophysical and biochemical microenvironmental cues including extracellular matrix (ECM) stiffness and dimensionality (2D and 3D)³. For example, the level of crosslinking of collagen in a dynamically stiffening ECM is a focal adhesion regulator in breast cancer tumorigenesis⁴. However, *in vitro* models to better-mimicking mechanotransduction mechanisms are still required to advance the study of breast cancer mechanobiology.

Biomaterial-based approaches with tunable stiffness and dimension present a unique opportunity to demonstrate the ECM mimetic modulatory effects of mechanical cues on selected cancer cell populations and their behaviors. For example, matrix stiffness of gastric cancer microenvironment was found as an epigenetic regulator of mechanotransduction-related YAP in a 3D collagen–alginate interpenetrating network (IPN)-based matrices, which were adjusted across a range of elastic moduli of gastric cancer tissues ($\sim 0.5 \text{ kPa} < G' < \sim 6.8 \text{ kPa}$)⁵. Varying migration patterns of breast cancer cells and metastasis responding changes in matrix stiffness were driven by gelatin-methacrylate hydrogels with stiffness ranging from soft to stiff (0.8 to 5 kPa)⁶. Oncogenic reprogramming of normal cells was displayed through 2D fibronectin-coated polyacrylamide hydrogels with varying stiffnesses (0.5 kPa, 1 kPa, 2 kPa, 4 kPa and 40 kPa), which resulted in RTK-*Ras* oncogenes to support mammary gland oncogenic reprogramming rely on YAP/TAZ. Additionally, pancreatic acinar cells in 3D gelatin-hyaluronan-based hydrogels (0.5 kPa and 9 kPa) were observed to support pancreatic tumorigenesis over *Ras*-mediated YAP/TAZ nuclear localization in response to matrix stiffening⁷.

Here, we investigate the plasticity of the metabolome of breast cancer cells in response to altering microenvironmental conditions. To this end, we developed 2D and 3D cell culture systems based on tyramine functionalized hyaluronic acid (HTA) hydrogels. The HTA hydrogels were cross-linked using horseradish peroxidase (HRP)-mediated oxidative coupling reaction as we previously demonstrated⁸. Hyaluronic acid (HA) is an integral molecular component of the breast cancer ECM and generally presents CD44 receptor, which is critical for cell adhesion, invasion, and mechanosensing. Therefore, HA-based hydrogels are suitable platform to investigate breast cancer cell behaviors⁹. Using this material platform, we demonstrated the possibility to modulate the breast cancer cells metabolome by tuning the mechanical properties and dimensions of HTA hydrogels (referred the mechano-metabolomics). A rigorous elucidation of changes in the metabolite profiles of MCF-7 cells and triple-negative MDA-MB-231 cells on 2D and in 3D HTA hydrogels having tunable matrix stiffness reveals that the cancer cells display differential metabolomic plasticity in response to changes in the matrix stiffness and dimension.

Materials and Methods

MDA-MB-231 and MCF-7 Breast Cancer Cell Cultures

MDA-MB-231 was kindly provided by Prof. Sedat Odabas (Ankara University, Turkey), and cultured in Dulbecco's Modified Eagle's Medium High Glucose (DMEM), with Fetal Bovine Serum (FBS, 10% v/v) and antibiotic–antimycotic solution (P/S, 1% v/v), in an incubator under 37 °C and 5% CO₂ conditions. The medium was refreshed every 2–3 days. MCF-7 cells (kindly provided by Prof. Ahmet Acar, Middle

East Technical University, Turkey) were cultured in DMEM with FBS (20% v/v) and P/S (1% v/v), in an incubator under 37 °C and 5% CO₂ conditions. The medium was refreshed every 2–3 days.

Preparation of HTA Gels with Differential Stiffness

Pure HTA powder (synthesized and characterized previously)¹⁰ was dissolved in Dulbecco’s Phosphate Buffer Saline (DPBS) at desired concentrations (1% and 5% wt.). HRP (2 U/mL) was added to the prepared pre-gel solutions to drive enzyme-mediated oxidative coupling reaction. Hydrogelation of 1% and 5% HTA pre-gels was triggered in well-plates by adding hydrogen peroxide (H₂O₂, 2mM) and incubation at room temperature for 1 min. After a washing step, cells were seeded on HTA hydrogels at the desired density. The cells were allowed to adhere to the materials for 30 min before top up the fresh media to ensure an effective cell adhesion. To prepare 3D cultures, HTA was added to wells, the cells were inoculated inside the gels, and H₂O₂ (2 mM) was injected to trigger instant gelation. Fresh media was added after the washing step. To monitor the effect of hydrogels on cell viability and proliferation, Live/dead staining and 2,3-Bis-(2-Methoxy-4-Nitro-5-Sulphophenyl)-2H-Tetrazolium-5-Carboxanilide (XTT) tests were performed with HTA (1% and 5% wt.) hydrogels before proceeding with the further experiments (details are provided in Supplementary Information).

Microstructural Characterizations of HTA Gels

Scanning electron microscopy (SEM) imaging was performed to examine the morphology and structure of 1% and 5% HTA hydrogels. HTA hydrogels were dehydrated by the critical point drying (CPD) method and then coated with gold/palladium. Images were obtained at 10 kV voltage and at different magnifications.

Ιμμνοστοαίνιγ φορ ΨΑΠ ανδ β-ακτιν

To visualize the breast cancer cell-matrix interaction and the response of cells to the matrix stiffness, we performed an immunofluorescent staining for β-actin (cell cytoskeleton protein) and mechanosensing protein YAP (see Supporting Information).

Gene Expression Study

The effect of matrix stiffness and context on MDA-MB-231 and MCF-7 cells were investigated at the molecular level by performing a reverse transcriptase-quantitative polymerase chain reaction (RT-qPCR) study (additional notes can be found in the Supplementary Information). The effect of matrix stiffness and matrix context on the expression of mechanotransduction markers in MCF-7 and MDA-MB-231 cells was examined by gene expression analyses of *YAP* , *TAZ* , *RhoA* and *FAK* .

Metabolomics

Metabolomics analysis was performed for MDA-MB-231 and MCF-7 cells, that were cultured on/in soft and stiff hydrogels, to specify the metabolites that alter in response to matrix stiffness and context. To this aim, MDA-MB-231 and MCF-7 cells (500.000 cells/gel) were seeded on/in hydrogels in well-plates, and the cell cultures were maintained for 3 days. At the end of the culture period, metabolomic analyses were performed as previously described (additional notes can be found in the Supplementary Information)¹¹ .

Drug testing

The cells (~50.000 cells/well, 96-well plate) were cultured for 48-hours to enable cell adhesion and stabilize the cell metabolism. Later, Doxorubicin (DOX, 0.2 µg/ml)¹² was applied in MDA-MB-231 and MCF-7 cells that were cultured on/in soft and stiff hydrogels. After DOX treatment for 72 h, an XTT test (Biological Industries, USA) was applied for MDA-MB-231 and MCF-7 cells to assess cell proliferation and chemoresistance on/in the gels. Absorbance values were recorded at 490 nm with a Multiskan Sky Microplate Spectrophotometer (Thermo Fisher).

Statistical analysis

Partial least squares-discriminant analysis (PLS-DA) was performed to reveal the discrimination between groups. Variable Importance in Projection (VIP) graphs were used to highlight the top 15 differentially expressed metabolites. Pathway analyzes were performed with the significantly altered metabolites (Student’s *t*-tests , $p < 0.05$) using MetaboAnalyst (<https://www.metaboanalyst.ca/ver.5.0>). The number of significantly differentiated metabolites between groups was illustrated on the Venn scheme and their names, pathways, and cellular locations were summarized in **Table S1** (dimensionality), **Table S2**(matrix stiffness in 2D), and **Table S3** (matrix stiffness in 3D). Gene expression and drug testing results were analyzed with One-way ANOVA and pairwise comparisons performed using Student’s *t*-tests , bars represent mean \pm SEM and symbols represent each experiment replicate, using GraphPad Prism 9 (for Windows, GraphPad Software, San Diego, California USA, www.graphpad.com).

Results and Discussion

The rationale of the study

The mechanometabolome of breast cancer was examined with MCF-7 (non-invasive) and triple-negative MDA-MB-231 (highly invasive) cell lines. Breast cancer was selected as a model in this work to represent an aggressive epithelial malignancy mediated by micro-environmental cues. In addition, it is well-known that breast tumor microenvironment undergoes a dynamic stiffening compared to healthy breast tissue (**Figure 1A**)¹³. The tumor-mimetic mechanical tunability of HTA was harnessed to create 2D and 3D matrices for breast cancer cells culture. The stiffness of breast tumors varies between 2 to 10 kPa *in vivo*. The tunable gelation of HTA enabled us to prepare hydrogels with controllable mechanical properties – ranging from soft (1% wt., ~ 1.95 kPa) to stiff (6% wt., ~ 9.6 kPa)⁸. SEM images of the hydrogels revealed a porous microstructure, as expected. Soft HTA hydrogels are characterized by a high density of interconnected large pores, while stiff HTA hydrogels are composed of compacted networks with narrow pores (**Figure 1B**). The different morphology of the dried hydrogels is indicative of the different physico-chemical properties determined by the range of concentration and crosslinking levels explored. Taken together, HTA is an ideal material candidate to investigate cell-material interactions and breast cancer mechanotransduction.

Assessment of cytotoxicity of HTA hydrogels for breast cancer cells

HA is one of the main components of breast tumor ECM⁶. To assess the potential applicability and toxicity of soft and stiff HTA hydrogels as cell culture scaffolds, MDA-MB-231 and MCF-7 breast cancer cells were cultured on the hydrogels for 2 and 5 days. We carried out a Calcein-AM/EtBr-1 double staining to visualize live cells as green stained and dead cells as red stained, as well as an XTT assay to further assess cell proliferation (**Figure S1**). Both MDA-MB-231 and MCF-7 cells were observed with low levels of dead cells. The proliferation of breast cancer cells was also promoted by HTA hydrogels (**Figure S1**).

Microscopic evaluation of the effect of stiffness and dimension on cell behavior

To assess the adhesion and morphologies of MDA-MB-231 and MCF-7 cells, the cells were monitored on the soft and stiff hydrogels in 2D and 3D culture systems on days 1 and 3 (**Figure 2A**). On the soft HTA hydrogels, MDA-MB-231 cells displayed a clustered morphology from day 1 to day 3, whereas a mixture of aggregated and adherent morphology were observed on stiff gels. Therefore, MDA-MB-231 cells assumed a more invasive morphology on the soft matrix, and a less invasive morphology on the stiffer matrix. On the other hand, MCF-7 cells exhibited a spread morphology on the soft HTA hydrogels whereas they assumed a clustered morphology on the stiff hydrogels after 3 days in culture (**Figure 2A**).

To monitor the cell morphology in 3D culture conditions, we encapsulated MDA-MB-231 cells and MCF-7 cells in both soft and stiff 3D hydrogels imitating native tumor ECM to characterize their mechanosensitive responses in the similitude of a native tumor ECM. Optical micrographs of MDA-MB-231 and MCF-7 cells embedded in the soft 3D hydrogels reveal an adherent character after day 1 and 3. It is noteworthy that a small number of tiny aggregates of MCF-7 were also observed in the soft hydrogels after day 3 in culture. On the other hand, MDA-MB-231 cells embedded within the stiff hydrogels formed spheroidal aggregates after day 3 in culture while MCF-7 cells predominantly assumed an adherent morphology with few clusters

(**Figure 2A**). The scanning electron micrographs further showed that both MDA-MB-231 and MCF-7 cells can adhere to soft and stiff hydrogels possibly owing to their inherent affinity for HA in the native tumor ECM⁹(**Figure 2B**); however, MDA-MB-231 cells were shown to tend to form aggregates while MCF-7 cells were more likely to adhere and grow filopodia.

We investigated the sensitivity of YAP in the breast cancer cells to increased stiffness. To this end, we performed immunostaining (YAP and β -actin) for breast cancer cells that were cultured on soft and stiff HTA hydrogels. Immunofluorescent images of the cells showed that YAP was spread throughout the cytoplasm of MDA-MB-231 and MCF-7 cells cultured on soft hydrogels, while it was accumulated around the nuclei of cells seeded on stiff hydrogels (**Figure 2C**). Cell aggregation was also visualized by β -actin staining on MDA-MB-231 and MCF-7 cells that were cultured on soft and stiff hydrogels. β -actin staining further confirmed that MDA-MB-231 and MCF-7 cells respond to matrix stiffness differently. The MDA-MB-231 cells form aggregates on stiff hydrogels while MCF-7 cells form a highly adherent morphology (**Figure 2C**).

Effect of matrix stiffness and dimension on mechano-related gene expressions

To determine mechanosensitive response of MDA-MB-231 and MCF-7 cells to changing matrix stiffness and dimension, we assessed the expressions of genes associated with mechanotransduction pathways in cancer cells using RT-qPCR. The expressions of *YAP*, *TAZ*, *RhoA*, and *FAK* genes were assessed after day 3 in culture. In MDA-MB-231 cells, the expression of *YAP* was elevated with the increasing stiffness in both 2D and 3D conditions (**Figure 3A**). Unlike in the 3D culture system where reduced expression of *YAP* was observed, *YAP* was highly expressed by MCF-7 cells in the 2D culture system as the hydrogel stiffness increases (**Figure 3B**). On the other hand, the expression of *YAP* in MCF-7 cells in 3D conditions was shown to decrease possibly due to the non-invasive character of the cells and the resulting relatively weak cell-ECM interaction.

The expression of *TAZ* gene by MDA-MB-231 cells in both our 2D and 3D culture systems was upregulated when the matrix stiffness was increased (**Figure 3A**), which might be the underlying reason for the enhanced cell proliferation in and on our hydrogel scaffolds (**Figure S1B**). *FAK* has a role as non-receptor tyrosine kinase providing signaling functions at the integrin binding sites, leading to cell migration. Our results showed that *FAK* expression was upregulated with increasing matrix stiffness in MDA-MB-231 and MCF-7 cells cultured in both 2D and 3D hydrogels (**Figure 3B**). In order to shed light on the role of *RhoA*, a member of *Rho*GTPases, in breast cancer, we investigated the effect of matrix stiffness on *RhoA* expression in our hydrogels. While we observed an upregulated expression of *RhoA* in the highly invasive MDA-MB-231 cells cultured on stiff 2D hydrogels, MCF-7 cells displayed a down-regulated expression of *RhoA* in the stiff 2D hydrogels. In contrast, MDA-MB-231 cells showed no significant alteration to the expression of *RhoA* in the stiff 3D hydrogels, whereas, the expression was upregulated in MCF-7 cells cultured under similar conditions (**Figure 3A and 3B**).

Evaluation of matrix stiffness and dimension on breast cancer cell metabolic plasticity

To examine the putative mechanisms of plasticity in breast cancer metabolome, we performed a comprehensive untargeted metabolomics analysis by GC-MS and LC-qTOF-MS. PLS-DA score plots showed clear discrimination between the metabolic phenotypes of both MDA-MB-231 (invasive) and MCF-7 (non-invasive) cells that were cultured in soft and stiff gels using 2D and 3D culture systems (**Figure 4Aa and 4Ba**). One-way ANOVA was further used to confirm the results(**Figure S2A and S2B**). This metabolic discrimination in MDA-MB-231 and MCF-7 cells was more significant in the stiff 2D matrix than the 3D counterpart. The most significantly altered 15 metabolites were reported in the VIP graphs (**Figure 4Ab and 4Bb**). For example, lysophosphatidylcholines (LysoPCs, LPC, a phospholipid), fucoxanthin, and phosphatidic acid (PA, a glycerophospholipid) were seen to be differentially expressed in the 2D system, while phosphatidylcholine (PC, a phospholipid), 4-cholesten-3-one, palmitoylcarnitine (a carnitine ester), and hexadecane (a hydrocarbon) were some of the main metabolites that were significantly altered in the 3D culture system with increasing matrix stiffness. The altered metabolites between MDA-MB-231 and MCF-7 cells cultured in soft

and stiff gels and in 2D and 3D conditions were further depicted in hierarchical cluster analysis (**Figure 4Ac and 4Bc**). A distinct pattern between the groups with high stiffness was observed. Strikingly, the levels of lysophosphatidylcholines were up-regulated in MCF-7 cells on soft gels (2D), while it was down-regulated in MDA-MB-231 in all conditions (2D and 3D, soft and stiff matrices) (**Figure 4Ac**). Similarly, D-Mannose, D-sphingosine, and cysteine were up-regulated in MDA-MB-231 cells on soft gels in 2D and down-regulated in 3D; as well as they were down-regulated in MCF-7 cells in all conditions. Importantly, the levels of phytosphingosine, dihydrosphingosine, C17-sphingosine, and 5-cholestan-3-beta were up-regulated commonly in both MDA-MB-231 and MCF-7 cells cultured within the soft hydrogels, whereas these metabolites were down-regulated in MDA-MB-231 and MCF-7 cells within the stiff hydrogel (**Figure 4Ac**). Pathway analysis showed that the altered metabolites mainly affected specific pathways including galactose metabolism, taurine hypotaurine and sphingolipid pathways in the 2D system whereas taurine hypotaurine metabolism, sphingolipid metabolism, glycerophospholipid metabolism, and arginine biosynthesis were affected in the 3D systems (**Figure 4C**). The metabolites that were significantly altered both in 2D and 3D were determined and illustrated in Venn diagram (**Figure 4D**). We established that 49 metabolites were commonly altered in both matrix dimensions (2D and 3D) and they are mainly associated with a fatty acid, phospholipid and sphingolipid metabolisms (**Table S1**). Hence, our data indicate that lipid metabolism-mediated matrix and membrane remodeling pathways were modulated independent of matrix dimensionality in breast cancer.

Investigation of the cell invasiveness on breast cancer mechano-metabolome

To specify the effects of matrix stiffness on individual breast cancer cell lines, we compared the metabolite profiles of each cell type in specific conditions (soft or stiff, 2D or 3D). The metabolic structure of MDA-MB-231 cells was affected by matrix stiffness, which is consistent with the PLS-DA results (**Figure S3A**). Similarly, MCF-7 cells responded to increased matrix stiffness (**Figure S3A**). The top 15 metabolites in discrimination between groups were provided in VIP plots (**Figure S3B**). Additionally, heat-maps of altered metabolites in MDA-MB-231 and MCF-7 cells on soft and stiff matrices were depicted with hierarchical cluster analyses (**Figure S3C**). The results were validated by t-tests (**Figure S4**).

To elaborate on the differentially regulated metabolites between groups, the up- and down-regulated metabolites, that created patterns on the heat-map analyses, were visualized on volcano plots (**Figure 5Aa**). We observed that various metabolites affecting the phospholipid biosynthesis, protein degradation and biosynthesis, and glycerophospholipid metabolism were up-regulated in MDA-MD-231 cells with the increased stiffness. In MCF-7 cells, fatty acid degradation (palmitocarnitine, L-acetyl carnitine), phospholipid biosynthesis (LPC, LysoPC), ECM amino acid remodeling (isoleucine, 5-methoxytryptophol) processes related metabolites were up-regulated with increased stiffness. The pathway impact analysis confirmed that cellular membrane and ECM remodeling-related lipid metabolism pathways were stimulated mostly in MDA-MD-231 cells with increasing stiffness in the 2D system (**Figure 5Ab**). Arginine biosynthesis, glycerophospholipid, TCA cycle and sphingolipid metabolism pathways were profoundly associated with cellular membrane and ECM-remodelling of the 2D culture of MDA-MB-231. In MCF-7 cells, phenylalanine-tyrosine-tryptophan, glycerophospholipid, and valine-isoleucine-leucine metabolism were the obvious pathways biased (**Figure 5Ab**). The Venn diagram revealed that 39 metabolites were commonly altered in both MDA-MB-231 and MCF-7 cells cultured on the 2D system (**Figure 5Ac**), and they were the active driver for phospholipid, glycerophospholipid and fatty acid metabolisms (**Table S2**).

Similarly, to reveal the effect of matrix stiffness in 3D conditions on the metabolomics structure of the various types of breast cancer cells examined, we compared the metabolite profiles of both MDA-MD-231 and MCF-7 cells cultured in soft and stiff matrices. The metabolic structures of MDA-MD-231 and MCF-7 cells were affected by matrix stiffness in the 3D culture system, which is in agreement with the PLS-DA results (**Figure S5A**). The top 15 metabolites in discrimination between groups were provided in VIP plots (**Figure S5B**), while the metabolomic discriminations were represented in heat-maps with hierarchical cluster analyses (**Figure S5C**).

Volcano plot obtained for MDA-MB-231 cells that compares the metabolite profiles of cells cultured in soft and stiff gels showed that piperidinecarboxaldehyde, phosphatidylcholine, calcipotriol, glutamylglycine, and

monoacylglyceride (18:2(9Z,12Z)/0:0/0:0) were mostly up-regulated in the stiff matrix. With MCF-7 cells, 4-cholesten-3-one, L-acetyl carnitine, citramalic acid, palmityl carnitine, D-sphingosine, and phosphatidylcholines were some of the up-regulated metabolites driven by high matrix stiffness (**Figure 5Ba**). These up-regulated metabolites significantly altered selected pathways including the linoleic acid, alpha-linoleic acid metabolism, and valine isoleucine biosynthesis pathways (**Figure 5Bb**). In the MCF-7 cells, valine, leucine and isoleucine, aminoacyl-tRNA, and arginine biosynthesis pathways were affected by the increased matrix stiffness in 3D culture (**Figure 5Bb**). Venn diagram revealed that 17 metabolites were significantly altered in common for MDA-MB-231 and MCF-7 cells with increasing matrix stiffness and in 3D culture conditions (**Figure 5Bc**), and they mainly affect the arginine and proline metabolism (**Table S3**).

Differential matrix parameters bring about the metabolic reprogramming in breast cancer tumor progression and malignancy

To investigate the effects of matrix stiffness and dimension on metabolomic plasticity and the possible effects of plasticity on tumour progression, we constructed pathway impact diagrams. Our findings show breast cancer cells in the 2D conditions undergo a set of modulations in the glucose, lipid, and energy metabolisms in response to increasing matrix stiffness (**Figure 4C**). On the other hand, modulation in amino acid metabolism accompanied by altered lipid and energy metabolisms was observed in the 3D culture system (**Figure 4C**). When we compared MDA-MB-231 and MCF-7 cells in the 2D system, sphingolipid metabolism, arginine biosynthesis, and citrate cycle were elucidated as varied in MCF-7 cells that differentiate predominantly through aromatic amino acid and branched amino acid metabolism pathways. Lastly, our results showed that MDA-MB-231 and MCF-7 cells within the hydrogels with the high stiffness displayed an induced amino acid metabolic reprogramming.

Effect of matrix stiffness and dimension on anti-cancer drug response

Tumor microenvironment mechanical cues also play a crucial role in not only promoting tumorigenesis but also chemoresistance. To examine the effect of matrix stiffness and matrix context on the chemotherapeutic response of breast cancer cells, MDA-MB-231 and MCF-7 cells were cultured on/in soft and stiff HTA hydrogels for 2 days, then treated with a widely used anti-cancer drug Doxorubicin (0.2 $\mu\text{g}/\text{ml}$) for 72 hours (**Figure 6A**). MDA-MB-231 and MCF-7 cells showed a higher chemoresistance and increased cell viability against doxorubicin after 72-hour of drug treatment in stiff hydrogels compared to soft hydrogels. Both cell lines respond to increasing stiffness. We observed increased cellular viability of MDA-MB-231 cells in 2D (soft=47%, stiff=55%) and in 3D (soft=51.1%, stiff=83%) hydrogels with increasing stiffness. Similarly, the cellular viability of MCF-7 cells was seen to increase with the increasing matrix stiffness both in 2D (soft=65%, stiff=96.8%) and 3D (soft=23.4%, stiff=41.7%) (**Figure 6B**). Evidently, the ECM stiffness could control the chemosensitivity of breast cancer cells and poor disease prognosis¹⁴.

Discussion

In this work, we aimed to reveal an unmet question so far, which is how matrix conditions, i.e., stiffness and dimension, affect cancer metabolome. Such a correlation provides opportunities to dissect fundamental information on the potential roles of metabolomics plasticity in tumour progression, as well as it may help develop drugs considering tumour matrix conditions to be more efficient.

To this goal, we first assessed the effects of matrix stiffness on the morphological characters of invasive (MDA-MB-231) and non-invasive (MCF-7) cells on 2D culture. We observed that MDA-MB-231 cells formed clusters on soft matrix and a mixture of adherent and clustered cells were observed on stiff matrix (**Figure 2A**). Whereas, MCF-7 cells depicted a spread morphology on soft matrix and clustered morphology on stiff matrix (**Figure 2A**). This observation was an indicative of a barely invasive morphology on the soft matrix and a more invasive morphology on the stiff matrix. This is consistent with previous studies which reported on how cell spreading regulates proliferation, apoptosis, invasion, and metastasis¹³ in a broad range of cancer cell type including lung carcinoma cells¹⁵, colorectal cancer cells¹⁶ and breast cancer cells¹⁴.

Solid tumors display a 3D architecture of cancer cells, non-cancer cells and ECM. In light of this, 3D

hydrogel systems have been extensively used to recapitulate the architectural and functional framework of various tumor microenvironments¹⁷. MDA-MB-231 cells were seen to display an adherent and clustered morphology in soft and stiff matrix, respectively, while MCF-7 cells exhibited an adherent character both in the soft and stiff matrix (**Figure 2A**). Put to gather, we can conclude that increasing matrix stiffening in 3D condition promotes malignant phenotype, which resembles *in vivo* tumor progression.

The transcriptional regulator YAP is modulated in several cancer types as a universal mechanotransducer¹⁸. To consolidate our inverted phase-contrast microscope observations, we performed an immunofluorescent study to investigate YAP expressions in breast cancer cells on soft and stiff 2D hydrogels. As expected, YAP was seen to be distributed across cytoplasm in the cells seeded on soft hydrogels, whereas it was seen to be accumulated around nucleus when the cells seeded on stiff hydrogels (**Figure 2C**). Our observation is consistent with a previously published study that reports nuclear YAP accumulation in mammary epithelial cells on a dynamically stiffening matrix¹⁹. Gene expression study (**Figure 3A, B**) further concretized the immunofluorescent results and are consistent with previous reports²⁰. According to established knowledge, low expression of *YAP gene*, which is a tumor suppressor, is generally associated with high malignancy²¹. Thus, suggesting that MDA-MB-231 cells displayed malignant tumor-related mechanosensitive response on the stiff 2D hydrogel as observed. Upregulated expression of TAZ-protein and activity promotes cell proliferation, and EMT in breast cancer²². In addition, upregulated expression of *FAK* in epithelial cancer has previously been recognized as an active driver of tumor invasiveness²³. Clearly, our assessments of the gene expression profile of the examined breast cancer cell lines showed how the heterogenous cell populations in a tumor microenvironment can display differential expression of hub genes related to mechano-transduction including *YAP*, *TAZ*, *FAK*, and *RhoA* in matrix stiffness and dimension-dependent manner.

Metabolic reprogramming is a key process in tumorigenesis²⁴. Particularly, the deregulation of fatty acid and amino acid anabolic/catabolic pathways have an impact on the metabolic regulation of tumor growth^{25,26}. We determined that increasing matrix stiffness modulate glucose, lipid, and energy metabolisms in 2D. While, modulation in amino acid metabolism and altered lipid and energy metabolisms was observed in the 3D culture conditions (**Figure 4C**). It is well-known that tumor growth and progression are closely associated with three main metabolic pathways – glucose metabolism, lipid metabolism, and amino acid metabolism, that also control tumor cell proliferation, survival and malignancy²⁵⁻²⁸. The malignant proliferation of tumor cells presents rapid glycolysis (Warburg effect) in different environments²⁸. Glucose metabolism is required for proliferating cancer cells that have a high demand for energy²⁹. The altered metabolites and metabolic pathways in both 2D and 3D conditions have effects on cell proliferation (see Supplementary Information), tumor progression, and increased malignant phenotype mediated high matrix stiffness.

In addition, we compared the metabolomics differences between MDA-MB-23 and MCF-7 cells cultured either in 2D or 3D. In 2D, sphingolipid metabolism, arginine biosynthesis, and citrate cycle were seen to be altered in MCF-7 cells (**Figure 4C**). Sphingolipids are responsible for cell adhesion and migration³⁰, while the citrate cycle metabolic pathway is related to the growth and invasion of cancer cells. In addition, arginine can modulate metastasis and anti-apoptotic signaling pathways in cancer cells^{31,32}. Therefore, it can be concluded that increasing the invasion and metastasis of MDA-MB-231 cells on hydrogels by increasing the stiffness of the substrate is expected. In 3D, both in MCF-7 and MDA-MB-231, increasing stiffness was found to induce amino acid metabolic reprogramming. This reprogramming is known to modulate cellular proliferation³³, epigenetic modifications³⁴, tumor growth³⁵, in either MCF-7 or MDA-MB-231 cells. In addition, an aberrant aminoacyl-tRNA biosynthesis and arginine biosynthesis in MCF-7 cells can be linked to tumor growth and metastasis, respectively³⁶. Moreover, linoleic acid and alpha-linoleic metabolism reprogramming might be responsible for an increased malignant phenotype of MDA-MB-231 cells²⁷.

It is known that TME has a critical role in the efficacy of anti-cancer drug response³⁷. We have seen that MDA-MB-231 and MCF-7 cells responded to increasing matrix stiffness in both 2D and 3D conditions, and showed a higher chemoresistance to the introduced anti-cancer drug, doxorubicin (**Figure 6**). This change in chemo-sensitivity is in strict correlation with metabolism. Metabolic reprogramming has a causative effect on signaling and proliferative inputs that characterize the resistance of cancer cells³⁸. Lipids are involved in

signal transduction and regulation of cell growth, proliferation, differentiation, survival, apoptosis, membrane homeostasis, motility, and drug resistance in cancer. Tumor metabolic reprogramming, dysregulation of lipid metabolism and oncogenic signaling enhance lipid biosynthesis to supply the building blocks for membrane formation and maintain the high proliferation rate of cancer cells, leading to increased drug resistance³⁹. Thus, the increased drug resistance observed in MCF-7 and MDA-MB-231 breast cancer cells in our stiff 2D and 3D systems can be linked to the altering lipid metabolism. In addition to lipid metabolism, reprogramming in the amino acid metabolism has previously been shown to play crucial roles in tumor growth and survival and resistance to anti-cancer drugs⁴⁰. Thus, particularly in our stiff and 3D condition, the increased chemoresistance can be associated with altering amino acid metabolism.

Disclosure statement: The authors declare no competing interests.

Contributions: B.D. and B.S. developed the concept and designed the experiments. B.S. performed the experiments and analyzed the data. B.S., C.C.E., and E.N. accomplished metabolomics analyses. M.D. supervised the hyaluronic acid-based experiments. B.S and B.D. wrote the paper. B.D. and B.O.O. edited and commented on the manuscript. All authors approved the final version of the manuscript.

References

1. Riehl, B. D., Kim, E., Bouzid, T. & Lim, J. Y. The role of microenvironmental cues and mechanical loading milieus in breast cancer cell progression and metastasis. *Frontiers in Bioengineering and Biotechnology* **8**, (2021).
2. Tse, J. M. *et al.* Mechanical compression drives cancer cells toward invasive phenotype. *Proceedings of the National Academy of Sciences* **109**, 911–916 (2011).
3. Romani, P., Valcarcel-Jimenez, L., Frezza, C. & Dupont, S. Crosstalk between mechanotransduction and metabolism. *Nature Reviews Molecular Cell Biology* **22**, 22–38 (2020).
4. Levental, K. R. *et al.* Matrix crosslinking forces tumor progression by enhancing integrin signaling. *Cell* **139**,891–906 (2009).
5. Jang, M. *et al.* Matrix stiffness epigenetically regulates the oncogenic activation of the yes-associated protein in Gastric cancer. *Nature Biomedical Engineering* **5**, 114–123 (2020).
6. Vasudevan, J., Lim, C. T. & Fernandez, J. G. Cell migration and breast cancer metastasis in biomimetic extracellular matrices with independently tunable stiffness. *Advanced Functional Materials***30**, 2005383 (2020).
7. Panciera, T. *et al.* Reprogramming normal cells into tumour precursors requires ECM stiffness and oncogene-mediated changes of cell mechanical properties. *Nature Materials* **19**,797–806 (2020).
8. Derkus, B. *et al.* Multicomponent hydrogels for the formation of vascularized bone-like constructs in vitro. *Acta Biomaterialia***109**, 82–94 (2020).
9. Rezaeeyazdi, M., Colombani, T., Eggermont, L. J. & Bencherif, S. A. Engineering hyaluronic acid-based cryogels for CD44-mediated breast tumor reconstruction. *Materials Today Bio* **13**, 100207 (2022).
10. Loebel, C., D’Este, M., Alini, M., Zenobi-Wong, M. & Eglin, D. Precise tailoring of tyramine-based hyaluronan hydrogel properties using DMTMM conjugation. *Carbohydrate Polymers* **115**,325–333 (2015).
11. Isik, M. *et al.* Mechanically robust hybrid hydrogels of photo-crosslinkable gelatin and laminin-mimetic peptide amphiphiles for neural induction. *Biomaterials Science* **9**,8270–8284 (2021).
12. D’Souza, A. M. *et al.* Small molecule CJOC42 improves chemo-sensitivity and increases levels of tumor suppressor proteins in hepatoblastoma cells and in mice by inhibiting oncogene gankyrin. *Frontiers in Pharmacology* **12**, (2021).
13. Acerbi, I. *et al.* Human breast cancer invasion and aggression correlates with ECM stiffening and immune cell infiltration. *Integrative Biology* **7**, 1120–1134 (2015).
14. Wei, S. C. *et al.* Matrix stiffness drives epithelial–mesenchymal transition and tumour metastasis through a twist1–G3BP2 mechanotransduction pathway. *Nature Cell Biology***17**, 678–688 (2015).
15. Yuan, Y., Zhong, W., Ma, G., Zhang, B., Tian, H. Yes-associated protein regulates the growth of human non-small cell lung cancer in response to matrix stiffness. *Molecular Medicine Reports***11**,

- 4267–4272 (2015).
16. Krndija, D. *et al.* Substrate stiffness and the receptor-type tyrosine-protein phosphatase alpha regulate spreading of colon cancer cells through cytoskeletal contractility. *Oncogene* **29**,2724–2738 (2010).
 17. Li, Y. & Kumacheva, E. Hydrogel microenvironments for cancer spheroid growth and drug screening. *Science Advances* **4**, (2018).
 18. Zanconato, F., Cordenonsi, M. & Piccolo, S. Yap and Taz: A signalling hub of the tumour microenvironment. *Nature Reviews Cancer***19**, 454–464 (2019).
 19. Lee, J. Y. *et al.* Yap-independent mechanotransduction drives breast cancer progression. *Nature Communications* **10**,(2019).
 20. Yuan, M. *et al.* Yes-associated protein (YAP) functions as a tumor suppressor in breast. *Cell Death & Differentiation***15**, 1752–1759 (2008).
 21. Scott, K. E., Fraley, S. I. & Rangamani, P. A spatial model of yap/taz signaling reveals how stiffness, dimensionality, and shape contribute to emergent outcomes. *Proceedings of the National Academy of Sciences* **118**, (2021).
 22. Cordenonsi, M. *et al.* The hippo transducer taz confers cancer stem cell-related traits on breast cancer cells. *Cell***147**, 759–772 (2011).
 23. Lahlou, H. *et al.* Mammary epithelial-specific disruption of the focal adhesion kinase blocks mammary tumor progression. *Proceedings of the National Academy of Sciences* **104**,20302–20307 (2007).
 24. Yue, X. *et al.* Leukemia inhibitory factor drives glucose metabolic reprogramming to promote breast tumorigenesis. *Cell Death & Disease* **13**, (2022).
 25. Han, J., Li, Q., Chen, Y. & Yang, Y. Recent metabolomics analysis in tumor metabolism reprogramming. *Frontiers in Molecular Biosciences* **8**, (2021).
 26. Warburg, O. On respiratory impairment in cancer cells. *Science***124**, 269–270 (1956).
 27. Wei, Z., Liu, X., Cheng, C., Yu, W. & Yi, P. Metabolism of amino acids in cancer. *Frontiers in Cell and Developmental Biology***8**, (2021).
 28. Koundouros, N. & Poulogiannis, G. Reprogramming of fatty acid metabolism in cancer. *British Journal of Cancer* **122**,4–22 (2019).
 29. Fong, M. Y. *et al.* Breast-cancer-secreted Mir-122 reprograms glucose metabolism in premetastatic niche to promote metastasis. *Nature Cell Biology* **17**, 183–194 (2015).
 30. Hannun, Y. A. & Obeid, L. M. Sphingolipids and their metabolism in physiology and disease. *Nature Reviews Molecular Cell Biology***19**, 175–191 (2017).
 31. Martínez-Reyes, I. & Chandel, N. S. Mitochondrial TCA cycle metabolites control physiology and disease. *Nature Communications* **11**, (2020).
 32. Patil, M. D., Bhaumik, J., Babykutty, S., Banerjee, U. C. & Fukumura, D. Arginine dependence of tumor cells: Targeting a chink in cancer’s armor. *Oncogene* **35**, 4957–4972 (2016).
 33. Tönjes, M. *et al.* BCAT1 promotes cell proliferation through amino acid catabolism in gliomas carrying wild-type IDH1. *Nature Medicine* **19**, 901–908 (2013).
 34. Sun, L., Zhang, H. & Gao, P. Metabolic reprogramming and epigenetic modifications on the path to cancer. *Protein & Cell***13**, 877–919 (2021).
 35. Son, J. *et al.* Glutamine supports pancreatic cancer growth through a KRAS-regulated metabolic pathway. *Nature***496**, 101–105 (2013).
 36. Ullah Khan, S. & Ullah Khan, M. The role of amino acid metabolic reprogramming in tumor development and immunotherapy. *Biochemistry and Molecular Biology* **7**, 6 (2022).
 37. Li, Y. *et al.* Matrix stiffness regulates chemosensitivity, stemness characteristics, and autophagy in breast cancer cells. *ACS Applied Bio Materials* **3**, 4474–4485 (2020).
 38. Morandi, A. & Indraccolo, S. Linking metabolic reprogramming to therapy resistance in cancer. *Biochimica et Biophysica Acta (BBA) - Reviews on Cancer* **1868**, 1–6 (2017).
 39. Germain, N. *et al.* Lipid metabolism and resistance to anticancer treatment. *Biology* **9**, 474 (2020).
 40. Yoo, H.-C. & Han, J.-M. Amino acid metabolism in cancer drug resistance. *Cells* **11**, 140 (2022).

Figures

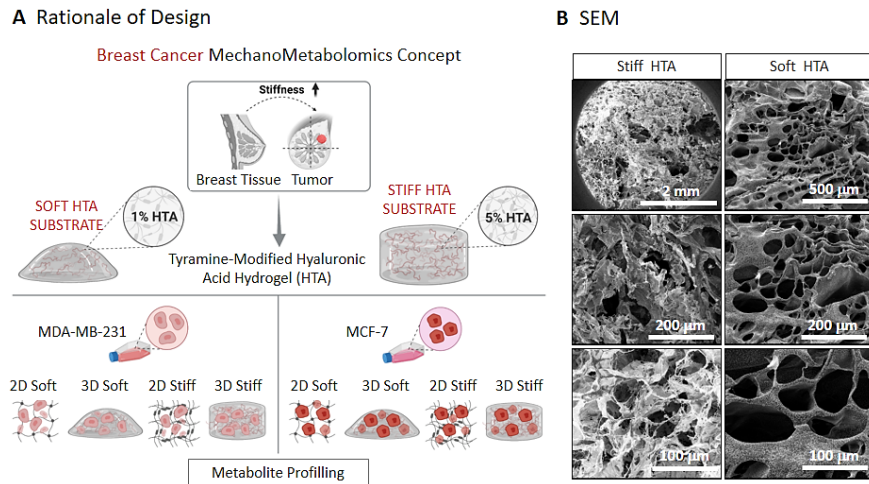


Figure 1

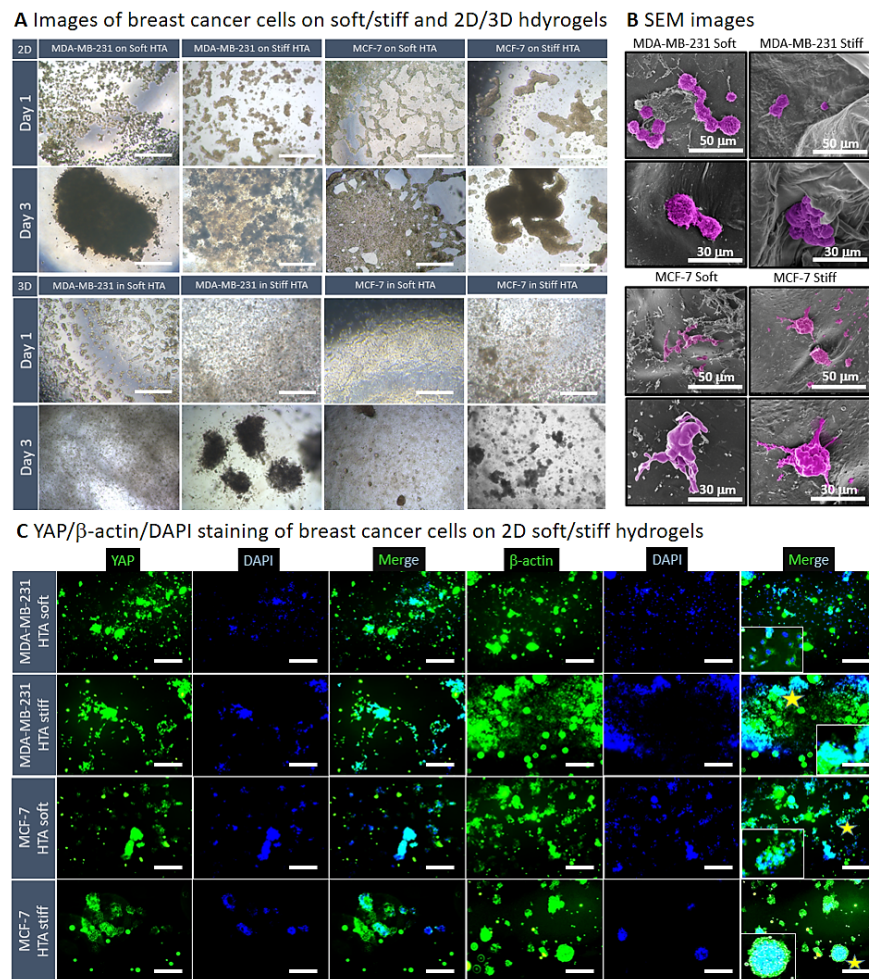


Figure 2

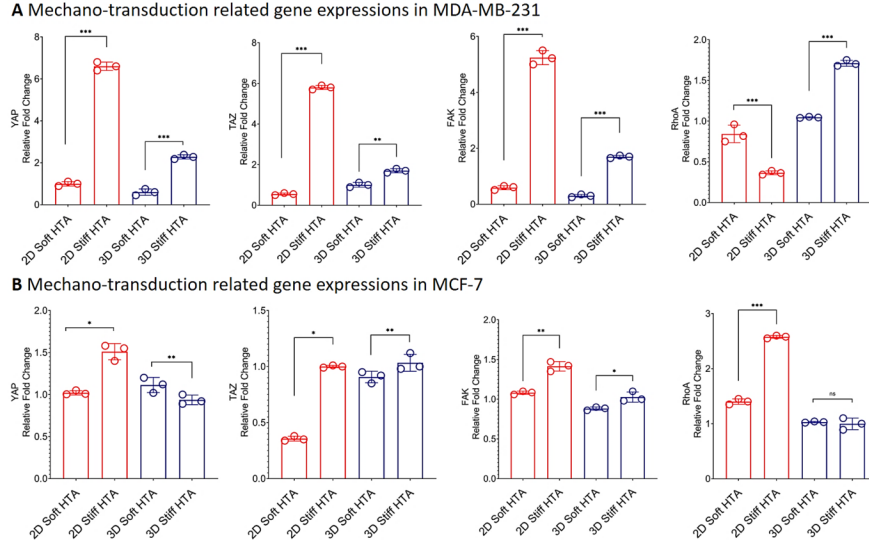


Figure 3

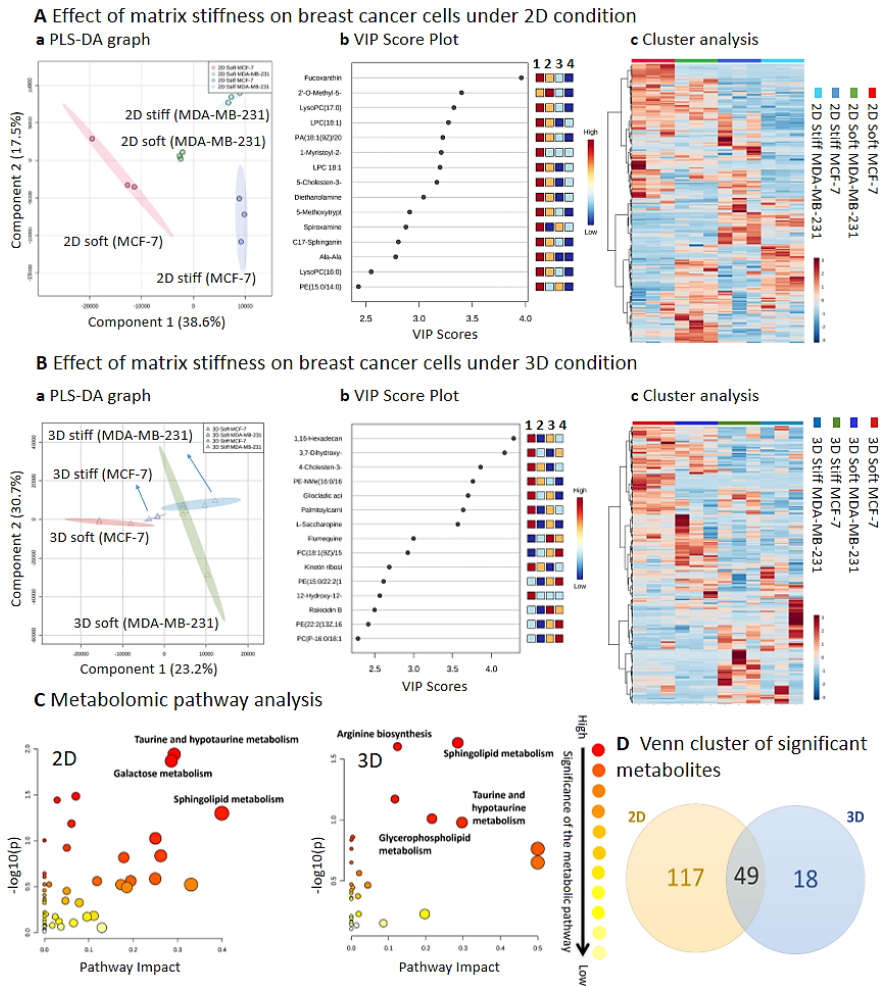


Figure 4

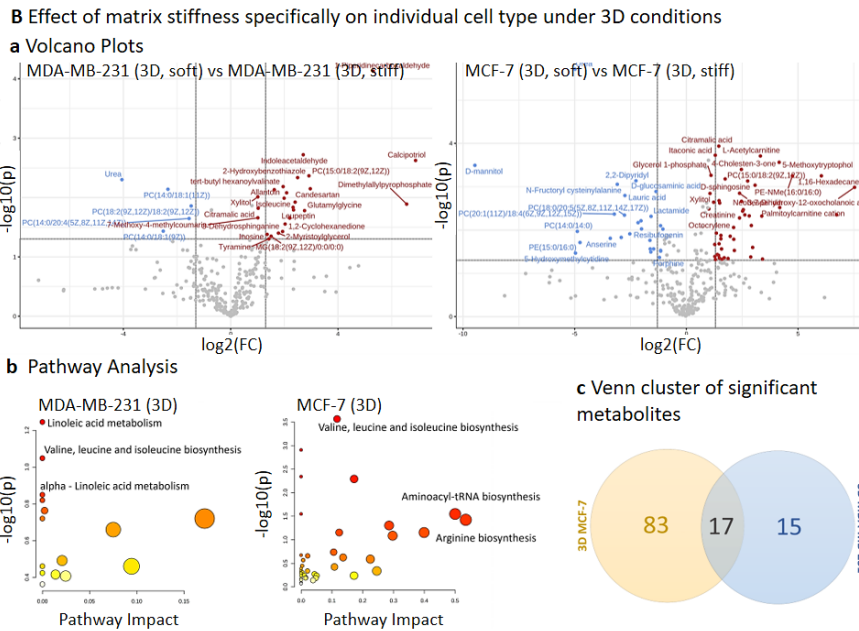
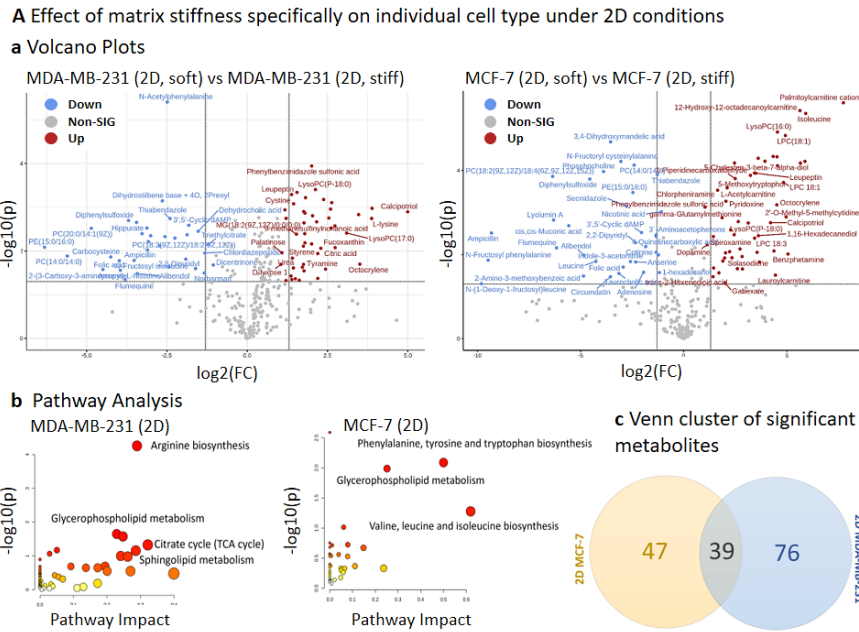


Figure 5

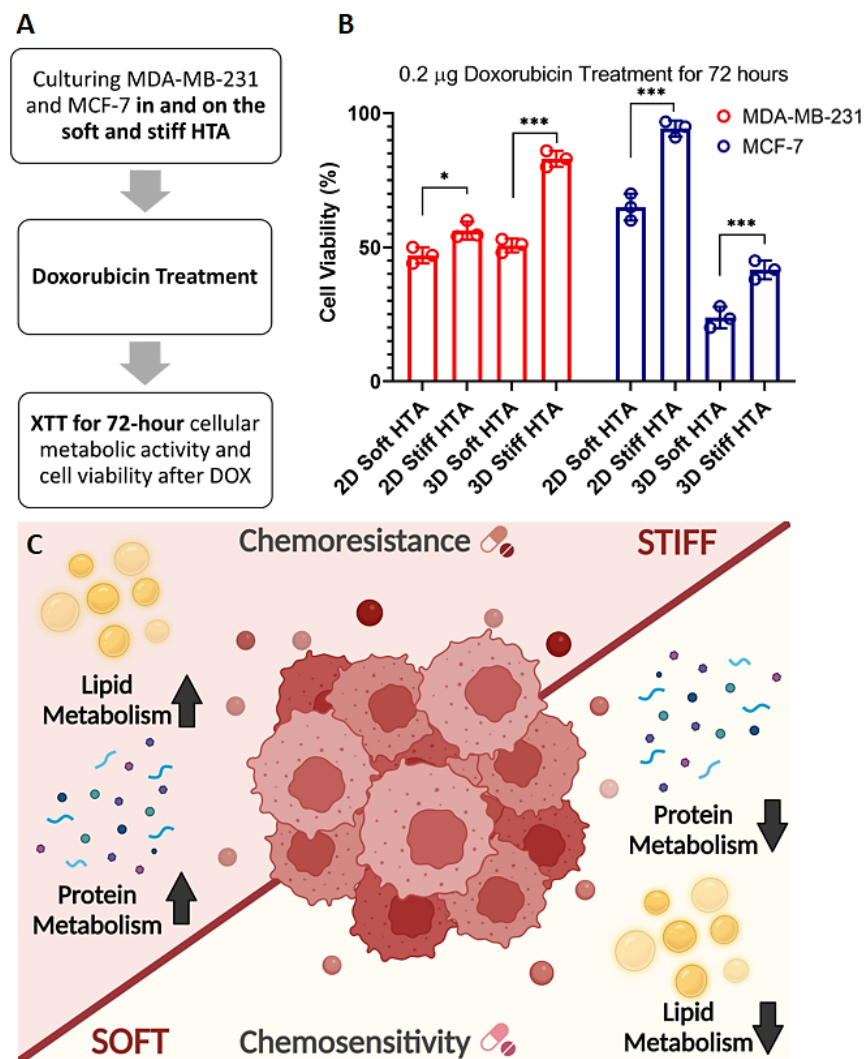


Figure 6

Figure Legends

Figure 1. (A) Mechanometabolomics concept was built on the culture of MDA-MB-231 and MCF-7 breast cancer cell lines in/on the soft and stiff HTA hydrogels. The effect of matrix stiffness and dimension on the cancer cell metabolism were tested using GC-MS/LC-qTOF-MS based metabolomics study. (B) Microstructural images of the soft and stiff HTA hydrogels.

Figure 2. Microscopic evaluation of the effect of stiffness and dimension on the behavior of breast cancer cells. (A) Inverted microscope images of MDA-MB-231 and MCF-7 cells on/in soft and stiff HTA gels (scale bars 200 µm). (B) SEM images of MDA-MB-231 and MCF-7 cells on soft and stiff HTA hydrogels with different magnifications. (C) IF images showing the expression of YAP (green), as well as the morphology of cells by β -actin (green). DAPI (blue) was used for nuclear counterstaining (scale bars 200 µm).

Figure 3. Gene expression analyses of mechano-related genes in MDA-MB-231 and MCF-7 cells on/in hydrogels . (A) The expressions of *YAP* , *TAZ* , *Rhoa* and *FAK* in MDA-MB-231 cells on/in

soft and stiff HTA hydrogels. (B) The expressions of *YAP*, *TAZ*, *RhoA* and *FAK* in MCF-7 cells on/in soft and stiff HTA hydrogels. Error bars denote Mean \pm SD for three independent experiments (biological replicate=3, technical replicate=3), p-significance as determined by Student's t-test (** $p < .0001$, ** $p < .001$, * $p < .05$).

Figure 4. Metabolic plasticity of MDA-MB-231 and MCF-7 cells in different matrix conditions (Biological replicate=3, technical replicate=3). (A and B) Effect of matrix stiffness on breast cancer cells in 2D and 3D conditions: (a) PLS-DA score plots that represents metabolomics discrimination between MDA-MB-231 (soft, Green), MCF-7 (soft, Pink), MDA-MB-231 (stiff, Violet), and MCF-7 (stiff, Turquoise). (b) VIP score plot indicating the top 15 most significant metabolites in discrimination between the groups, $p < 0.05$ as determined by one-way ANOVA. (c) Heat-map with hierarchical clustering analysis obtained by altered metabolites in MDA-MB-231 and MCF-7 cells in soft and stiff gels in 2D culture. (C) Pathway impact analysis representing the affected metabolic pathways by stiffness-mediated differentially expressed metabolites in 2D and 3D conditions. (D) Venn scheme summarizing the significantly altered metabolites in 2D and 3D conditions.

Figure 5. Mechano-metabolomic analyses (biological replicate=3, technical replicate=3). (A) Effect of matrix stiffness specifically on individual cell type under 2D and 3D conditions: (a) Volcano plots demonstrating the significantly up- and down-regulated metabolites in MDA-MD-231 and MCF-7 cells on soft and stiff matrices. (b) Pathway impact analyses representing the affected metabolic pathways by differentially expressed metabolites in MDA-MD-231 and MCF-7 cells on soft and stiff matrices. (c) Venn scheme summarizing the altered and common metabolites MDA-MD-231 and MCF-7 cells on soft and stiff matrices. $n=3$ and * $p < 0.05$ as determined by Student's t-test.

Figure 6. DOX anti-cancer drug testing. (A) The representative scheme of doxorubicin anti-cancer drug treatment experimental design. (B) Anti-cancer drug (0.2 $\mu\text{g}/\text{ml}$ DOX, 72h) response of MDA-MB-231 and MCF-7 cells in 2D and 3D, soft and stiff gels ($n=3$). Percentage cell viability was presented. Error bars denote Mean \pm SD for three independent experiments, p-significance as determined by Student's t-test (** $p < .001$, ** $p < .01$, * $p < .05$). (C) An illustration explaining the synergistic effects of matrix stiffness, dimension, and metabolomic plasticity on the anti-cancer drug sensitivity of breast cancer cells.